STUDY OF THERMAL STRATIFICATION AND MIXING USING PIV

B. Yamaji, R. Szijártó, A. Aszódi

Institute of Nuclear Techniques, Budapest University of Technology and Economics

Abstract

Paks Nuclear Power Plant uses the REMIX code for the calculation of the coolant mixing in case of the use of high pressure injection system while stagnating flow is present. The use of the code for Russian type WWER-440 reactors needs strict conservative approach, and in several cases the accuracy and the reserves to safety margins cannot be determined now. In order to quantify and improve these characteristics experimental validation of the code is needed.
An experimental program has been launched at the Institute of Nuclear Techniques with the aim of investigating thermal stratification processes and the mixing of plumes in simple geometries. With the comparison and evaluation of measurement data and CFD results computational models can be validated.
For the experiments a simple hexahedral plexiglas tank (250x500x100 mm – HxLxD) was fabricated with five nozzles attached, which can be set up as inlets or outlets. With different inlet and outlet setups and temperature differences thermal stratification, plume mixing may be investigated using Particle Image Velocimetry.
In the present paper comparison of PIV measurements carried out on the plexigas tank and the results of CFD simulations will be presented. For the calculations the ANSYS CFX was used.

1. INTRODUCTION

Several publications investigate coolant mixing in pressurized water reactors, WWER-440 reactors (Rohde et al. 2007) or thermal stratification in the primary circuit (Boros and Aszódi, 2008). The understanding of these processes is fundamental from nuclear safety point of view. In Hungary Paks Nuclear Power Plant applies the REMIX code (Iyer et al., 1986) for the analysis of Emergency Core Cooling System (ECCS) operation and thermal stratification. For the verification of the models applied in REMIX a program was started to experimentally and numerically investigate such phenomena. Thermal stratification has been investigated in other cases both experimentally (Hunt et al., 2001) and numerically (Zachár and Aszódi, 2007). In this paper experimental investigation of thermal stratification using Particle Image Velocimetry (PIV) (Raffel et al., 2007) and the applied measurement setup will be presented together with the comparison of measurement data and computational results. For three-dimensional Computational Fluid Dynamics (CFD) calculations ANSYS CFX 11.0 commercial code (ANSYS, 2006) was used.
For the measurements a rectangular plexiglas tank was designed based on analyses of Pressurized Thermal Shock (PTS) scenarios of WWER reactors (AEKI, 2005). The tank has five nozzles that can be set up as inlets or outlets. With the help of the auxiliary system different coolant temperatures and mass flow rates can be set.

2. EXPERIMENTAL SETUP AND COMPUTATIONAL MODELS

2.1 Measurement Setup

Flow and plume behaviour and thermal stratification were investigated in a rectangular plexiglas tank. The tank has a removable top and five nozzles that can be set as inlets or outlets. Dimensions and the location of the five nozzles (N0-N4) are shown in Figure 1. Nozzle T indicates the location where the thermocouple line was inserted.

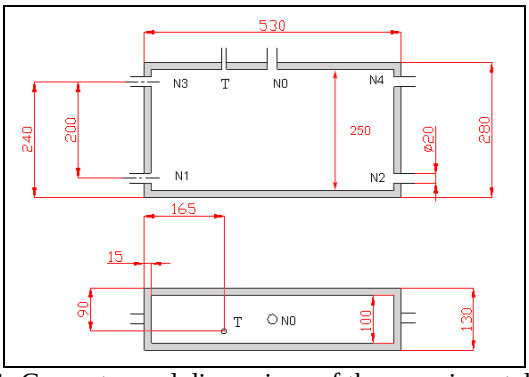

Fig. 1. Geometry and dimensions of the experimental tank

Particle Image Velocimetry (PIV) is an optical measurement technique that enables the mapping of instantaneous velocity distributions within planar cross-sections of a flow field. The flow domain is seeded with small polyamide particles. The tracer particles are illuminated by a thin light sheet, generated from a double-cavity laser system. The light scattered by the particles is recorded on two subsequent image frames by a digital imaging device, typically a CCD camera. The velocity vectors are calculated from the displacement of the scattering particles based on the image pairs and the time delay between them. The images are analysed with cross-correlation techniques to calculate the velocity vectors (Raffel et al., 2007).

The PIV measurement system used for the experiments consists of a double cavity Nd:YAG pulsed laser (wavelength: 532 nm, maximum pulse energy: 135 mJ) with light sheet optics, a double frame CCD camera (resolution: 1600x1200 pixel) with a 60 mm lens and a band pass filter (532 nm), a timer a synchroniser and a computer. For seeding polyamide particles with 50 μm mean diameter were used.

Water supply of desired temperature (between 16°C and 80°C) and flow rate (between 0,001-0,1 kg/s) is provided by an auxiliary system shown in Figure 2. This system consists of electric water heaters, pipings, valves, a pump, flow regulators, thermometers and flow meters, pressure reductors and by-pass lines. The plexiglas tank is connected to the system with flexible pipes.

Fig. 2. Auxiliary system, experimental tank with laser and camera

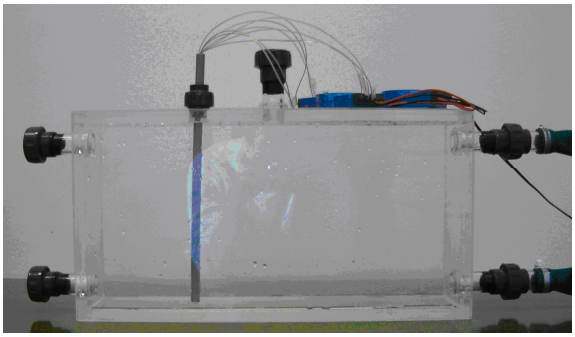
Fig. 3. Plexiglas experimental tank with inserted thermocouple line

A vertical thermocouple line of eight thermocouples was inserted into the tank at location T shown in Figure 1. Measurement of thermal stratification was done with this thermocouple line. The plexiglas tank with the inserted thermocouple line is shown in Figure 3.

Analysis and processing of recorded PIV data was performed using the commercial software package Dantec Dynamics V3.00 (Dantec, 2008).

2.2 Measurement Configuration

A series of measurements were carried out in order to investigate temperature stratification and plume behaviour. The five nozzles of the tank can be used as inlets or outlets, therefore a plenty of configurations can be set up. With the variation of water flow rate and temperature a large matrix of measurements can help this investigation. In the following two measurements (D6 and D8) will be presented. In these cases nozzle N0 was used as inlet and nozzles N1 and N2 were outlets (see Figure 1 and Figure 4). Cold water is injected through the inlet into stagnating hot water.

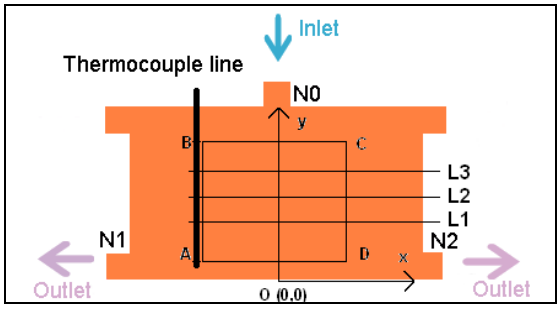

Fig. 4. Boundary conditions of the measurements,
location of the thermocouple line, detected area and monitor lines

In Figure 4 rectangle A-B-C-D represents the location of the area detected by PIV. Coordinates of the rectangle for cases D6 and D8 are shown in Table 1. Three monitor lines were defined for the quantitative analysis of the flow maps, L1 is located at 1/4 height of the detected area, L2 is at 1/2 height and L3 is at 5/8 height. Table 1 summarizes the initial and boundary conditions and the absolute coordinates of the detected area and the monitor lines in case of measurements D6 and D8. In the first case (cold) inlet temperature was slightly higher than in the second case, but the initial (hot) average temperature in the tank was about 8°C lower (D6: 39.47°C, D8: 46.945°C), therefore the temperature difference was greater in case of D8. The inlet mass flow rate was almost identical for the two cases.

Table 1. Measurement boundary conditions, position of detected area and monitor lines

	D6	D8
Inlet temperature – T_{in} [°C]	20	16
Inlet mass flow rate – m_{in} [g/s]	34	35
Inlet	N0	N0
Outlets	N1, N2	N1, N2
Initial average temperature – $T_{0,av}$ [°C]	39.47	46.945
Location of detected area – X,Y coordinates [m]		
A	-0.096, 0.02	-0.085, 0.019
B	-0.096, 0.23	-0.085, 0.227
C	0.179, 0.23	0.19, 0.227
D	0.179, 0.02	0.19, 0.019
Location of monitor lines – Y coordinate [m]		
L1	0.0725	0.071
L2	0.125	0.123
L3	0.15125	0.149

Initial vertical temperature distributions are shown in Figure 5. Table 2 shows the coordinates of the thermocouples. The accuracy of the thermocouples is ±1°C therefore the distributions are close to uniform. During the transients sampling frequency of the thermocouple line was 1 Hz. Functions were fitted on the initial thermocouple data to provide initial conditions for the CFX calculations (highlighted as T(y) in Figure 5). During measurement D6 thermocouple TC6 did not operate properly, in this case it did not register temperature data.

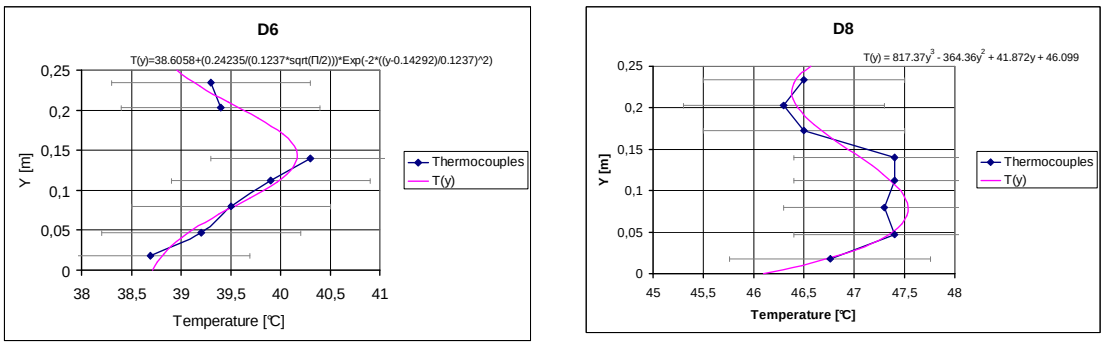

Fig. 5. Initial vertical temperature distribution and the functions used in CFX

Table 2. Coordinates of the thermocouples

Thermocouple	TC1	TC2	TC3	TC4	TC5	TC6	TC7	TC8
Y [m]	0.018	0.047	0.08	0.112	0.14	0.173	0.203	0.234

The transients started with the opening of the inlet valve and the opening of the two outlet valves. Using flow regulators the outlets were set to be symmetrical, i.e. the outlet flow rate was the same at the two outlets. Duration of the transients was 40 s. This length was enough to investigate the basic phenomena applying constant inlet mass flow rate boundary condition. The PIV measurements started together with the opening of the outlet valves. Image pairs were recorded at a rate of 10 Hz, time delay between two images was set to 10 ms. The two-dimensional measurements of the flow field were done in the greater vertical symmetry plane (X–Y symmetry plane) of the tank. The laser was positioned in such a way that the laser light sheet entered the tank between nozzles N1 and N3. The camera was positioned perpendicular to the light sheet.

2.3 Computational Model of the Measurements

Computational Fluid Dynamics calculations of the presented measurement configurations were performed. The three-dimensional simulations were carried out using ANSYS CFX 11.0.
A three-dimensional model of the plexiglas tank was built using hexahedral volumetric mesh. The model includes the main flow domain (i.e. the tank with the five nozzles). Inlet and outlet boundary conditions were set at the cross-sections of the selected nozzles, walls are defined as no-slip adiabatic walls (the heat loss through the walls of the tank was neglected in the CFD calculations). The thermocouple line is not included in the computational model. The geometry includes all five nozzles. Depending on the problem, for different simulations front faces of selected nozzles were set as inlets, outlets or walls. Figure 6 and Figure 7 show the geometry of the CFX model, and the hexahedral volumetric and surface mesh.

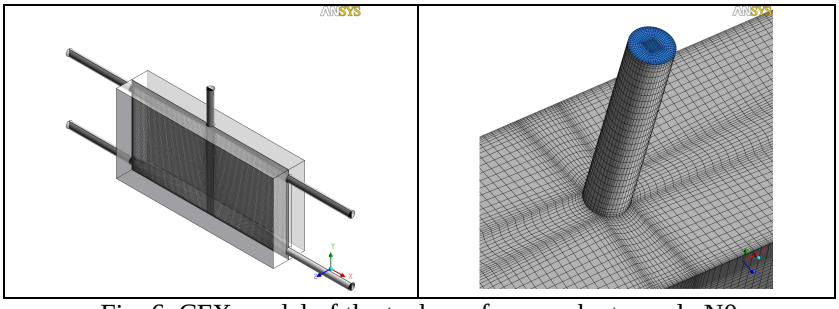

Fig. 6. CFX model of the tank, surface mesh at nozzle N0

Figure 7 shows a representation of the volumetric mesh in the X–Y symmetry plane of the model. The model had 1.09 million hexahedral volumetric elements and 1.138 million nodes.

For each measurement transient calculations were carried out using two different turbulence models: shear stress transport (SST) and SSG Reynolds stress model. For inlet boundary condition mass flow rate was defined, for outlet boundary condition zero relative pressure was set. Initial vertical temperature distribution was defined by functions shown in Figure 5 according to the thermocouple line measurements. The total simulation time was set to 40 s, and the time step was Δt=0.2 s. Table 3 shows the parameters of the presented calculations.

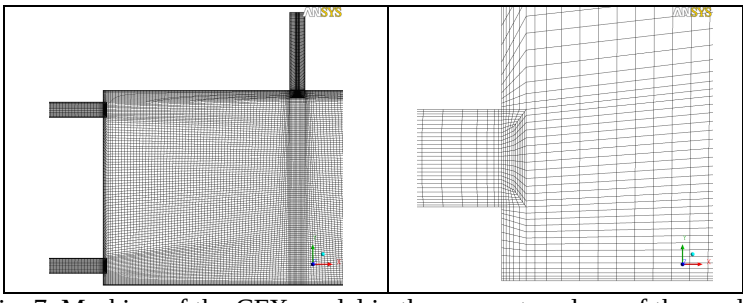

Fig. 7. Meshing of the CFX model in the symmetry plane of the model

Table 3. Parameters of simulations for case D6 and D8

Simulation	Turbulence model	Inlet turb. intensity	Inlet mass flow rt. [g/s]	Inlet temp. [°C]	Simulation time [s]	Time step [s]
D6SSG05	SSG	5%	34	20	40	0.2
D6SSG10	SSG	10%				
D6SST05	SST	5%				
D6SST10	SST	10%				
D8SSG05	SSG	5%	35	16		
D8SSG10	SSG	10%				
D8SST05	SST	5%				
D8SST10	SST	10%				

3. MEASUREMENT RESULTS AND COMPARISON WITH SIMULATIONS

3.1 Velocity Field

PIV measurement records the instantaneous velocity field. For t=10s, t=20s, t=30s and t=40s these field can be seen in Figure 8, left column. The image recording frequency was 10 Hz during the transients. Figure 8 gives a detailed picture about the flow behaviour in time (measurement D8). Vortices form near the plume, these vortices propagate along the plume and detach. The originally stagnating domain generally moved toward the plume, and where vortices formed, the region with lower velocities turns and separates into upward and downward flow. The plume fluctuates near the centreline of the inlet nozzle. In order to investigate the general processes an average field for each second was calculated using the instantaneous field plus the four preceding and the four succeeding fields. For example for t=10s the average field was produced by averaging the field of t=9.6s, t=9.7s, … t=10.3s and t=10.4s. The average fields (see Figure 8, right column) are smoothed but still carry the general characteristics of the flow field. Figure 9 shows the calculated temperature and velocity fields at different time values for simulation D8SST10. The plume can be clearly indentified in the velocity field. It is also significant that these simulations did not reproduce the vortices and the fluctuations of the plume. However, the calculated velocity values were in very good accordance with the values of the average fields. In Figure 9 the black rectangle in the field maps symbolises the boundaries of the detected area of the PIV measurement. Crosshairs in the temperature maps symbolise the location of the thermocouples (for locations of the thermocouples see Figure 1, Figure 4 and Table 2). The horizontal flow (X direction) further from the plume, in the lower half of the tank in the simulations is

very similar to the measured flow field. In the following values of the one-second-average velocity fields will be compared to the CFX results.
Quantitative comparison of the measurement and the four CFX simulations were done using the vertical (Y direction) component (V) distribution at monitor lines L1 and L3 as shown in Figure 10 and Figure 11.

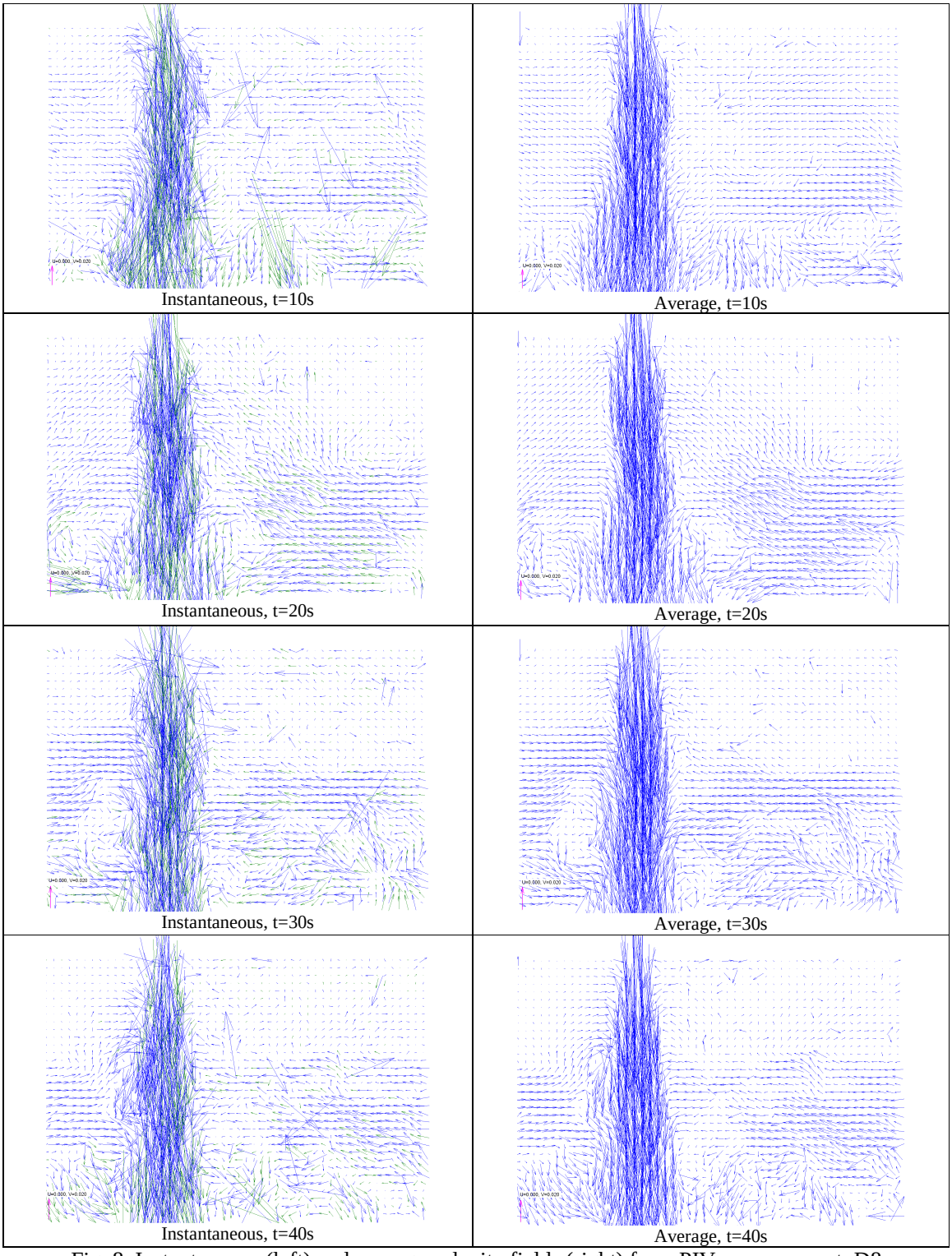

Fig. 8. Instantaneous (left) and average velocity fields (right) from PIV measurement, D8

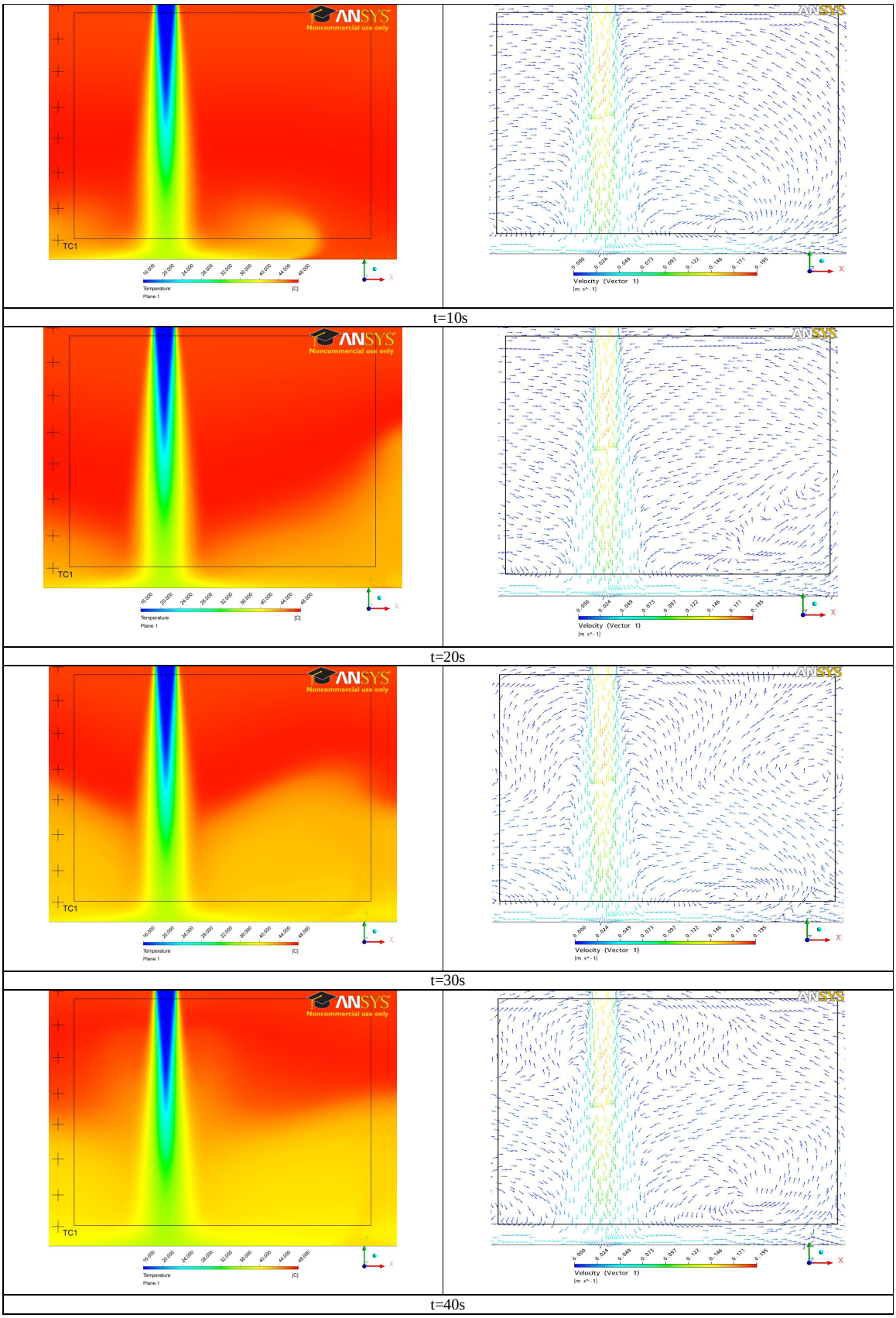

Fig. 9. Calculated temperature and velocity field, D8SST10

In Figure 10 and Figure 11 red line graphs with markers show the measured values. Generally, the simulations reproduced the location and the width of the plume well. Calculations using the SSG turbulence model over predicted the velocity values, the deviation of maximum values varies between 10-30%. Results of SST calculations are in very good agreement with the measurements, especially in the lower part (i.e. monitor line L1) of the tank. In the upper half the SST simulations over predicted the velocity as well, but the deviation is less. It is also visible that the difference between 5% and 10% turbulence intensity at the inlet has practically negligible effect on the results, but still larger turbulence intensity gives slightly better results.

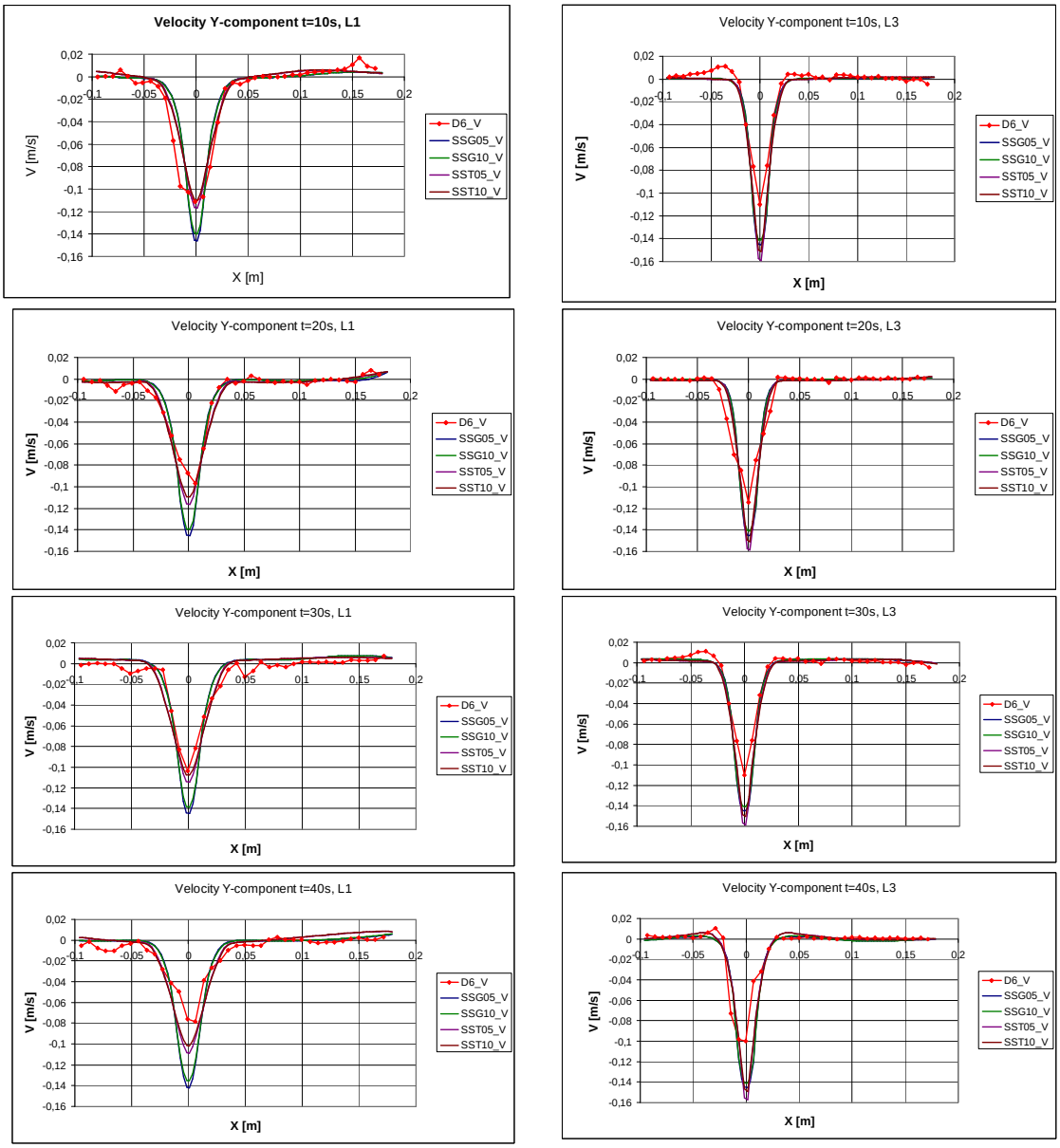

Fig. 10. Vertical velocity component at monitor lines L1 and L3, compared with simulations, D6

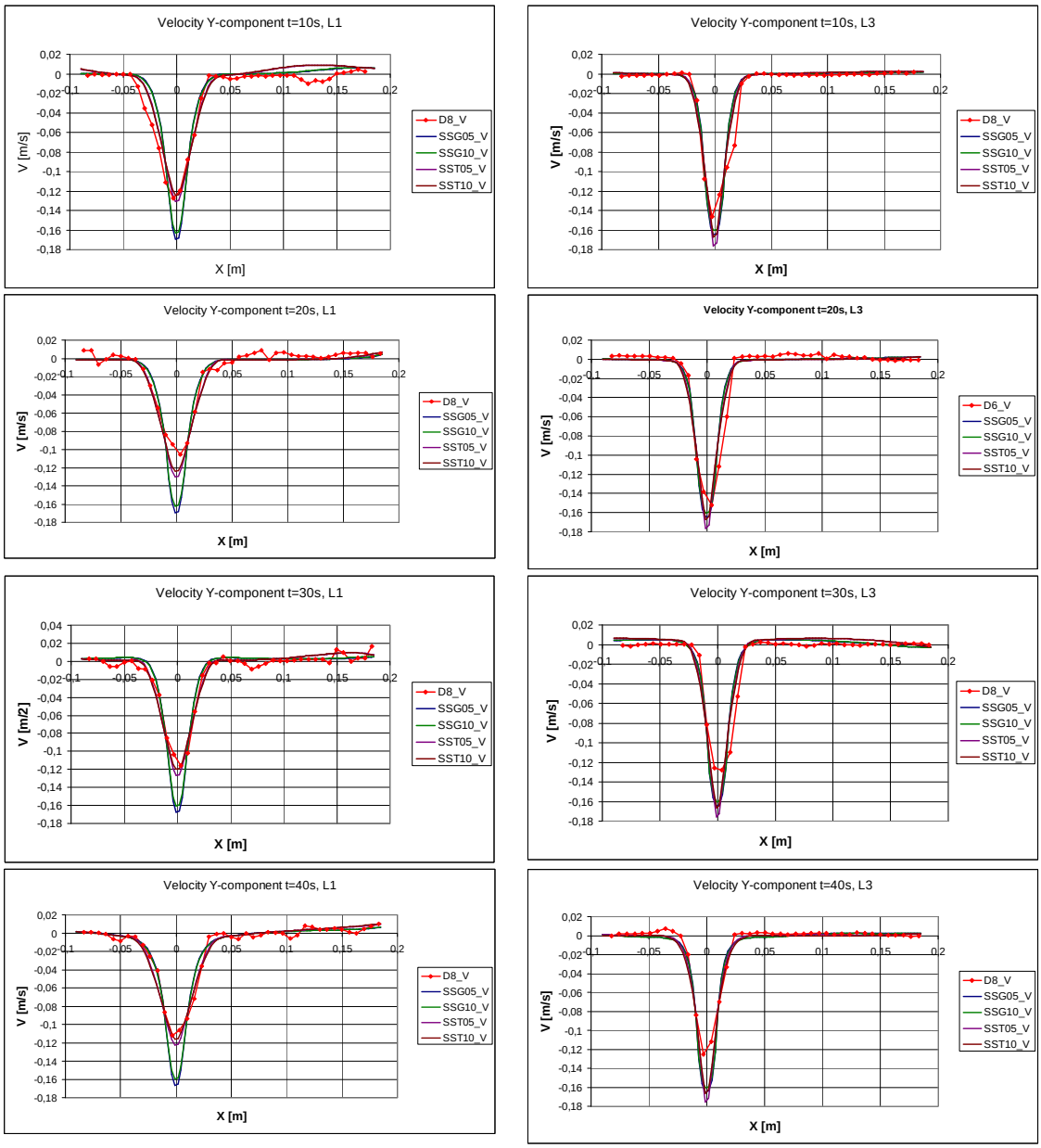

Fig. 11. Vertical velocity component at monitor lines L1 and L3, compared with simulations, D8

3.2 Temperature Stratification

Figure 12 shows the temperature detected by three thermocouples (TC8 (top), TC5 and TC1 (bottom)) during the transients for case D6 and D8. For the exact location of the thermocouple line and the thermocouples see Figure 1, Figure 4 and Table 2.

Compared to the results of the CFX calculations it is visible that the general behaviour was reproduced well with CFX. In most part of the transient the calculated values are within the range of the thermocouples, and follow the measured trends. In case of measurement D8, during the last ten seconds of the transient the simulations under predicted the temperature at the thermocouples, but it is only significant in the lower part of the tank, where the temperature decrease was significant. It is also visible that – outside the cold jet – there is practically no change in temperature in the upper part of the tank. This effect can be seen also in the calculated temperature fields (see Figure 9).

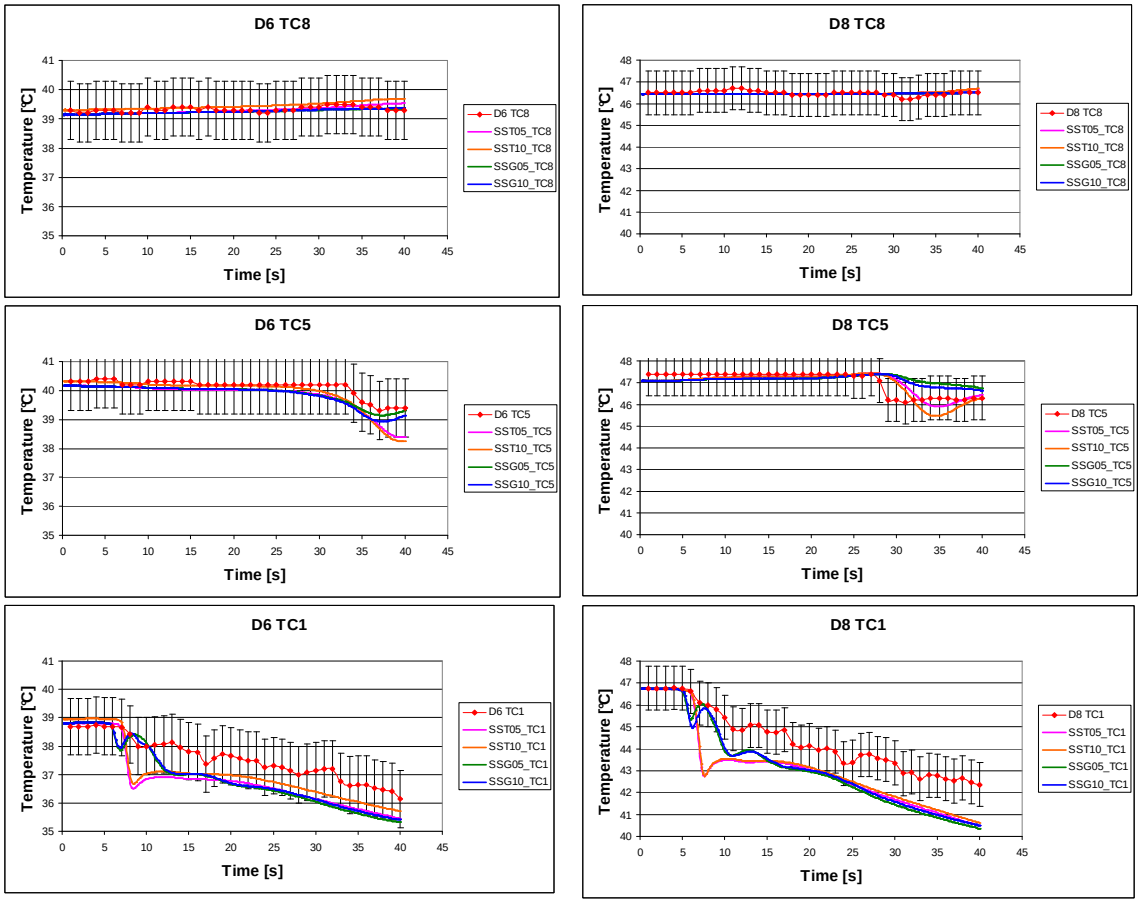

Fig. 12. Temperature (TC8 (top), TC5 and TC1 (bottom)) compared with results of the CFX calculations (D6 and D8)

Figure 13 shows the vertical temperature distribution registered by the thermocouple line and is compared to the CFX results. As it is shown in Figure 12 and Figure 13 the CFX simulations under predicted the temperature in the lower part of the tank. Qualitatively the distributions are in good agreement. In the lower part (TC1-TC4) both the SST and SSG simulations produced values below the measured data. The difference between the measured and calculated values increases toward the end of the transient for both cases presented.

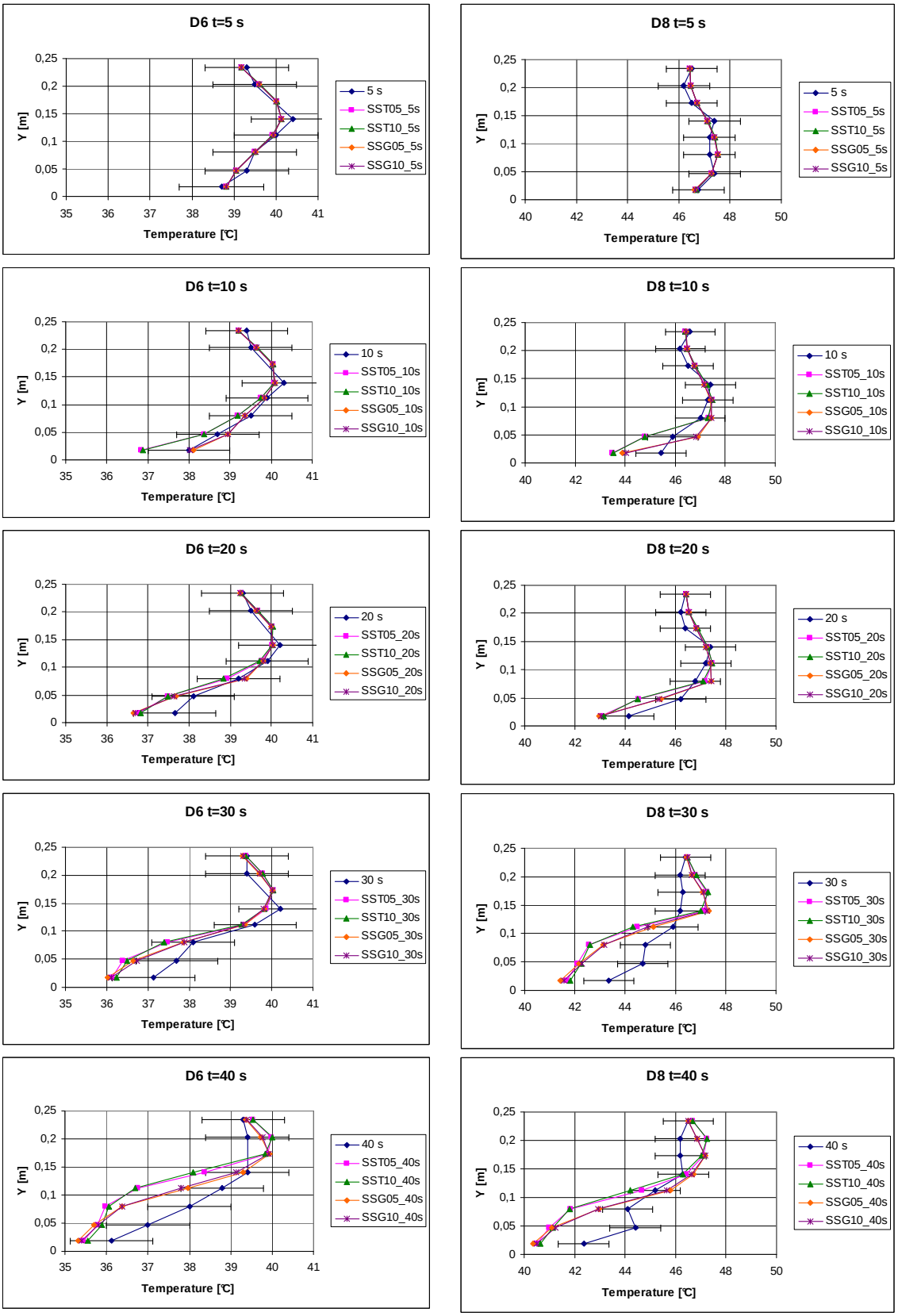

Fig. 13. Vertical temperature distribution at the thermocouple line and results of the CFX calculations

4. CONCLUSIONS

Experimental and numerical investigation of thermal stratification and plume mixing was presented. A series of experiments were carried out using PIV and thermocouple measurements, two selected measurements were presented and compared with CFD calculations. The applied CFX models reproduced the measured velocity distributions and temperatures relatively well.
For the improvement of the measurements, repeatability tests will have to be carried out. In case of the simulations further calculations are needed to test mesh and time-step independence.
Further investigations should include longer transients and the application of higher inlet mass flow rates and larger temperature differences. Simultaneous Laser Induced Fluorescence would also give a more detailed picture of the temperature distribution. From computational point of view better reproduction of instantaneous behaviour will be needed. That would help the better understanding of plume mixing as well.

REFERENCES

ANSYS CFX Release 11.0 Users' guide, ANSYS, 2006

I. Boros, A. Aszódi: "Analysis of Thermal Stratification in the Primary Circuit of a VVER-440 Reactor with the CFX Code", *Nuclear Engineering and Design*, 238, 453-459 (2008)

DynamicStudio – User's Guide, Dantec Dynamics, 2008

G.R. Hunt, P. Cooper, P.F. Linden: "Thermal stratification produced by plumes and jets in enclosed spaces", *Building and Environment*, 36, 871-882 (2001)

K. Iyer, H. P. Nourbakhsh, T. G. Theofanous: "REMIX: A Computer Program for Temperature Transients Due to High Pressure Injection After Interruption of Natural Circulation, NUREG/CR-3701, USA, (1986)

Thermal-hydraulic analyses of PTS scenarios, (In Hungarian) KFKI AEKI Atomic Energy Research Institute, Budapest, Hungary, 2005

M. Raffel, C. Willert, S. Wereley, J. Kompenhans: *Particle Image Velocimetry - A practical guide*, Springer, Berlin, Germany, 2007

U. Rohde, T. Höhne, S. Kliem, B. Hemström, M. Scheuerer, T. Toppila, A. Aszódi, I. Boros, I. Farkas, P. Mühlbauer et al.: "Fluid mixing and flow distribution in a primary circuit of a nuclear pressurized water reactor — Validation of CFD codes", *Nuclear Engineering and Design*, 237, 1639-1655 (2007)

A. Zachár, A. Aszódi: "Numerical Analysis of Flow Distributors to Improve Temperature Stratification in Storage Tanks", *Numerical Heat transfer*, 51, 919-940 (2007)